(4)

Office of Naval Research

Contract N00014-87-K-0738

Task No. 431a020

Technical Report No. 2

MORPHOLOGY OF ZnS PARTICLES PRODUCED FROM VARIOUS ZINC SALTS BY HOMOGENEOUS PRECIPITATION

by

Ahmet Celikkaya and Mufit Akinc

Prepared for Publication

in the

Journal of the American Ceramic Society

Iowa State University

Department of Materials Science and Engineering

Ames, Iowa 50011

December 14, 1988

SECURITY CLASSIFICATION OF THIS PAGE

REPORT DOCUMENTATION PAGE

1a. REPORT SECURITY CLASSIFICATION Unclassified	1b. RESTRICTIVE MARKINGS
2a. SECURITY CLASSIFICATION AUTHORITY	3 DISTRIBUTION / AVAILABILITY OF REPORT Approved for public release Distribution unlimited
2b. DECLASSIFICATION / DOWNGRADING SCHEDULE	
4. PERFORMING ORGANIZATION REPORT NUMBER(S) #2	5. MONITORING ORGANIZATION REPORT NUMBER(S) N00014-87-K-0738
6a. NAME OF PERFORMING ORGANIZATION Iowa State University Mufit Akinc 6b. OFFICE SYMBOL (If applicable)	7a. NAME OF MONITORING ORGANIZATION Office of Naval Research Dr. R. Schwartz
6c. ADDRESS (City, State, and ZIP Code)	7b. ADDRESS (City, State, and ZIP Code) Code 38504 Naval Weapons Center China Lake, CA 93555-6001
8a. NAME OF FUNDING / SPONSORING ORGANIZATION 8b. OFFICE SYMBOL (If applicable)	9. PROCUREMENT INSTRUMENT IDENTIFICATION NUMBER
8c. ADDRESS (City, State, and ZIP Code)	10. SOURCE OF FUNDING NUMBERS PROGRAM ELEMENT NO. / PROJECT NO / TASK NO. / WORK UNIT NO 4312020

11. TITLE (Include Security Classification)

Morphology of ZnS Particles Produced from Various Zinc Salts by Homogeneous Precipitation

12. PERSONAL AUTHOR(S)

Ahmet Celikkaya and Mufit Akinc

13a. TYPE OF REPORT	13b. TIME COVERED	14. DATE OF REPORT (Year, Month, Day)	15. PAGE COUNT
Technical	FROM _____ TO _____	88/12/14	26

16. SUPPLEMENTARY NOTATION

Submitted to Journal of the American Ceramic Society

17. COSATI CODES			18. SUBJECT TERMS (Continue on reverse if necessary and identify by block number)
FIELD	GROUP	SUB-GROUP	

19. ABSTRACT (Continue on reverse if necessary and identify by block number)

20. DISTRIBUTION / AVAILABILITY OF ABSTRACT ☐ UNCLASSIFIED/UNLIMITED ☐ SAME AS RPT ☐ DTIC USERS	21 ABSTRACT SECURITY CLASSIFICATION
22a. NAME OF RESPONSIBLE INDIVIDUAL	22b TELEPHONE (Include Area Code) / 22c. OFFICE SYMBOL

DD FORM 1473, 84 MAR 83 APR edition may be used until exhausted. All other editions are obsolete

SECURITY CLASSIFICATION OF THIS PAGE

MORPHOLOGY OF ZnS PARTICLES PRODUCED FROM VARIOUS ZINC SALTS BY HOMOGENEOUS PRECIPITATION

A. Celikkaya and M. Akinc

Department of Materials Science and Engineering

Iowa State University

Ames, Iowa 50011

This manuscript is prepared for publication in the

Journal of American Ceramic Society

ABSTRACT

Colloidal sols of ZnS were prepared by thermal decomposition of thioacetamide in acidic zinc solutions. Precipitation was carried out in the presence of nitrate, acetate, chloride and sulfate ions. Particle morphology was influenced by the chemical nature of the anions present in the solution as well as the rate of sulfide ion generation. Spherical, monodisperse particles having a specific type of particle size distribution, i.e., monosized, bimodal or continuous distribution, with mean sizes in the range of 0.15 μm to 3 μm, were formed depending on the anion type and sulfide ion generation rate. Individual particles always consisted of clusters of sphalerite crystallites except when sulfide ions were generated at low rates and sulfate ions were present. In such cases a mixture of α and β-ZnS were formed.

INTRODUCTION:

Over the past decade several researchers have produced colloidal sols of many hydrous oxides and sulfides consisting of particles having uniform size and shape. In addition to the commonly recognized variables such as pH, temperature and concentrations of various chemical reactants, the type of the electrolyte present can significantly affect system stability, particle morphology and composition of the precipitate through complex formation. Complexing of the precipitating cation with one or more of the anions present in the system, at varying strengths, may either limit the concentration of free cation in the solution or serve as an intermediate species contributing to the formation of a particular crystalline phase and/or particle morphology. Alternatively, those anions acting as a weak base may buffer the pH of the solution leading to similar results. It is also possible that these anions may be incorporated into the solid phase, affecting the composition of the precipitates.

Although considerable progress has been made in explaining various aspects of the precipitation phenomena, it is difficult to draw general conclusions from specific systems. However, demonstration of the ability to reproducibly prepare colloidal particles of a specific composition and morphology under various experimental conditions can lead to models which can lead to further understanding of the precipitation phenomenon.

Studies dealing with the synthesis and characterization of colloidal sols of oxides, carbonates, phosphates and their combinations are more common in the literature than those concerned with non-oxide salts such as sulfides, selenides and others. This is very probably due to toxicity problems and/or the sensitivity of the non-oxide reactants and products to air and water vapor (1,2). Wilhelmy and Matijevic (3) prepared spherical, micron sized β-ZnS particles by aging zinc ions in hot thioacetamide solution for several hours, with nitrate being the supporting anion. Williams et al. (4), on the other hand, used sulfate as the supporting anion to prepare 3 μm zinc sulfide spherical particles which were a mixture of the α and β forms. Williams et al. reported that the spheres were initially appeared as cubes of 1 μm size, while Wilhelmy and Matijevic observed 0.16 μm spherical "seeds" initially.

The primary purpose of the present study was to investigate the role of supporting anions on the kinetics of precipitation and on the morphology of the particles formed. To do this, zinc sulfide was precipitated by thermal decomposition of thioacetamide (TAA) in acidic aqueous solutions where sulfate, acetate, chloride and nitrate ions were employed as supporting anions.

Precipitation of zinc sulfide by thermal decomposition of TAA in acidic solutions is known to proceed as follows (5,6)

$$CH_3C(S)NH_2 \xrightarrow{H_3O^+} CH_3C(O)NH_2 + H_2S \qquad -\frac{d[TAA]}{dt} = k[H_3O^+][TAA] \quad (1)$$

$$H_2S \rightleftharpoons HS^- + H_3O^+ \qquad K_{a,1} = \frac{[HS^-][H_3O^+]}{[H_2S]} \quad (2)$$

$$HS^- \rightleftharpoons S^- + H_3O^+ \qquad K_{a,2} = \frac{[S^-][H_3O^+]}{[HS^-]} \quad (3)$$

$$Zn^{2+}(aq) + S^-(aq) \rightleftharpoons ZnS(s) \qquad Ksp = [Zn^{2+}][S^-] \quad (4)$$

Decomposition of TAA to yield hydrogen sulfide is the rate limiting step, and the decomposition kinetics has been studied in great detail (5). Using equations 1-3, the sulfide ion concentration at any time t can be estimated for any combination of pH, temperature and initial concentration of thioacetamide. Then, it is possible to determine the *supersaturation* S, *defined as*

$$S = \left(\frac{[S^-]_t[Zn^{2+}]}{K_{sp}}\right)^{1/2}, \quad (5)$$

at the instant of nucleation, where t is the observed time from the beginning of the experiment to the onset of nucleation, K_{sp} is the equilibrium solubility product of β-ZnS, $[Zn^{2+}]$ is the concentration of free zinc ions and $[S^-]_t$ is the concentration of sulfide ions at time t given by (7)

$$[S^-]_t = \frac{[TAA]_o(1-\exp(-k[H_3O^+]t))}{([H_3O^+]^2/K_{a,1}\,K_{a,2}) + ([H_3O^+]/K_{a,2}) + 1} \quad (6)$$

Thus one can estimate the degree of supersaturation for nucleation using equations (5) and (6).

EXPERIMENTAL:

A. Precipitation: Stock solutions of zinc acetate, zinc sulfate, zinc chloride and zinc nitrate (Fisher, Reagent Grade) were prepared by dissolving each salt in deionized water so as to produce a zinc ion concentration about 1.5 M. Solutions were filtered through 0.1 μm membranes and stored in polyethylene bottles. Cation stock solution and the conjugate acid of the supporting anion were added to a beaker in predetermined quantities along with a sufficient amount of distilled water to bring the total volume slightly less than 250 mL. The amount of the acid and cation stock solutions added were determined on the basis of desired pH and cation concentration. The acidic cation solution was heated to reaction temperature on a hot plate, and the predetermined amount of thioacetamide (Aldrich Chem. Co.) was dissolved in the solution. Solution volume was brought to exactly 250 mL, and the beaker containing the solution was placed in a water bath at the set reaction temperature. The time to onset of precipitation, manifested as the appearance of a bluish tint, was recorded for each experiment. Small aliquots were collected and quenched to 15°C at regular intervals to observe development of particle morphology and growth kinetics.

Initial zinc ion concentration, $[Zn^{2+}]_o$, was kept constant at 0.05 M in all experiments, while initial thioacetamide concentration was varied to give $[TAA]_o/[Zn^{2+}]_o$ ratios of 4, 8 and 16. Two levels of Solution pH obtained

with conjugate acids (pH = 1 and pH = 2). When the supporting anion was acetate, however, pH of the system remained constant at 1.9, possibly due to buffering action of the acetate ions with other ions in the solution.

B. Characterization: A centrifugal particle size analyzer* was employed for determination of size distribution using a portion of quenched aliquots. Remainder of each aliquot were centrifuged at 5000 rpm for 45 minutes. The recovered precipitates were then washed once with deionized water and once with acetone. During the acetone wash, particles were dispersed with a sonic disruptor+. A drop of suspension in acetone was placed on an aluminum foil and dried for observation of morphology by SEM‡. X-ray diffraction‡ patterns were obtained to determine the structure, mean crystallite size and phase purity of the powders. Organic contaminants were assessed from FTIR‡ spectra.

---

* Horiba Particle Size Analyzer, CAPA 700, Irvine, CA
+ Tekmar Sonic Disruptor, Tekmar Company, Cincinnati, OH
‡ JEOL Model 840A, JEOL Ltd. USA, Peabody, MA
‡ Siemens D500 Diffractometer, Siemens, Denver, CO
‡ IBM IR 98 FTIR Spectrophotometer, IBM Instruments, Inc., Danbury, CT

RESULTS AND DISCUSSION:

A. Effects of supporting anion on precipitation kinetics.

The critical supersaturation was determined for a number of combinations of experimental variables, and was found to have a value of about 10 for any combination of experimental variables. Figure 1a shows the change of supersaturation S with time plotted using equation 5 and 6 for temperature T = 60°C, initial thioacetamide concentration $[TAA]_o$ = 0.4 M, pH = 2, and initial zinc ion concentration $[Zn^{2+}]_o$ = 0.05 M, assuming that all zinc ions are free. On the same figure, the times to observe the onset of the precipitates are indicated with corresponding values of critical supersaturation for each anion system. The kinetics of the formation of spherical submicron ZnS particle with nitrate as the supporting anion has been previously reported (8). Since nitrate ions do not form strong complexes with Zn^{2+}(9), variations in precipitation kinetics and particle characteristics observed with other supporting anions were compared to those for nitrate in this study. Two possible explanations can be offered for the observed variation in the value of critical supersaturation for different anion systems. First, presence of a specific anion may effectively alter the solid-liquid interfacial energy which would cause the critical nucleus size to be different for each anion system. This is equivalent to saying that the critical supersaturation is indeed different for each anion system. Secondly, it is also possible that although the critical

supersaturation is the same for each anion system, nucleation starts at different times because a certain fraction of the initial zinc ions may be complexed by anions in the solution. Table I lists the formation constants for acetato, sulfato, chloro and nitrato complexes of zinc corrected for the ionic strengths of the solutions that we used (9). Complex species involving hydroxide ions were not considered since they are known not to be significant below pH = 3 (10), and all of our experiments were performed with pH at or below 2.

Taking into consideration the buffering effect of HSO_4^- and SO_4^{2-} ions at a pH of 2 and the expected complex formation reactions, we calculated that about 15% of the Zn^{2+} ions will be tied up by sulfate ions. Similar calculations indicate that only 4% of the Zn^{2+} ions will be complexed by nitrate ions, validating the assumption that nitrate can be considered inert in terms of complex forming ability. The predicted influence of sulfate complexing of zinc ion on the supersaturation with time is shown as curve b on Figure 1, where a 15% reduction in $[Zn^{++}]_o$ (from 0.050 M to 0.425 M) has been assured because of complexing. The time for critical supersaturation of $S \simeq 10$ is read from curve b as 13 min, which is slightly longer than that found experimentally. This small difference may be due to uncertainties involved in determining the exact time at which nucleation started; however, this analysis is consistent with the delay in nucleation for the sulfate system being due to lower free zinc ion concentration. Calculations for the chloride system

Table I Concentration equilibrium constants for acetato, nitrato, sulfato and chloro complexes of Zn^{2+} ions found by interpolation using Davies equation at corresponding ionic strengths of the solutions we used.

Formation Constant	Ligand (L^{-y})			
	SO_4^-	OAc^-	NO_3^-	Cl^-
$K_{f,1}$ $[ZnL_1]^{-y+2}$	12.58	11.22	0.66	2.32
$K_{f,2}$ $[ZnL_2]^{-2y+2}$	7.94	6.16	0.38	1.41
$K_{f,3}$ $[ZnL_3]^{-3y+2}$	0.70	1.23	--	0.89
$K_{f,4}$ $[ZnL_4]^{-4y+2}$	1.13	--	--	0.50

also supported this conclusion. Although stability constants for acetato complexes of zinc (Table I) are very close to those for sulfato complexes, nucleation is observed in the acetate system much earlier than for sulfate and even nitrate. Obviously, the presence of acetate ions either catalyses the thioacetamide decomposition or helps to reduce critical nucleus radius. The latter mechanism is possible if acetate reduces the surface energy of the nuclei or forms intermediate species that facilitate attachment of ions to subcritical nuclei. Figure 2 shows the variation of thioacetamide concentration with time. Curve a is obtained from equation 1 and curve b corresponds to experimentally measured values as determined by following the concentration of TAA at 261 nm by a UV-Vis spectrophotometer in the presence of zinc and acetate ions. The apparent sudden increase in TAA concentration measured experimentally is actually due to scattering by the formation of precipitate particles rather than to an abrupt change in TAA concentration. Since the experimental data follows the theoretical curve very closely prior to precipitation, the premise that the presence of acetate ions augments the rate of decomposition of TAA fails. FTIR spectra of ZnS powders prepared from acetate solutions did not contain any peaks indicating involvement of an intermediate species in the solid phase. Thus, it is difficult to explain the observed anomalously early nucleation from acetate solutions, and this phenomenon needs to be investigated in more detail.

B. Effect of supporting anion on particle morphology.

B.1. Nitrate system

The size distribution type and texture of particles varied considerably with the chemical nature of the supporting anions present and with the sulfide ion generation rate. As has been discussed, sulfide ion generation rate is a function of temperature, pH and initial concentration of thioacetamide, thus all of these variables determine the rate of approach to critical supersaturation. Since critical supersaturation was observed to be approximately the same for all experiments, the reciprocal of time at which nucleation was observed represents a sorted of averaged rate of approach to nucleation and will be referred to as "rate-to-nucleation". Rate-to-nucleation (RN) for various combinations of experimental variables for nitrate solutions are given in Table II. Below RN = 1.11×10^{-2} min^{-1}, it usually took exceedingly long times for precipitation to start (~3 hours) and agglomerates of particles were observed. However, depending on the relative value of RN above 1.11×10^{-12} min^{-1}, either monosized, bimodal or continuous distributions of particle sizes were obtained with the nitrate system. Monosized particles were observed for RN in the range of 1.11×10^{-2} min^{-1} to 1.00 min^{-1}, e.g. Fig. 3a. At intermediate RN values ($1.00 < RN < 1.50$ min^{-1}), bimodal particle size distributions were obtained; e.g. Figure 3b. At still higher RN values, continuous particle size

Table II - Variation of rate of sulfide ion generation with various combinations of experimental parameters for nitrate system. $[Zn^{2+}]_o$ = 0.05 M.

Temperature (°C)	pH	$[TAA]_o$	RN(min^{-1})
60	1	0.2	6.6×10^{-3}
60	1	0.4	1.41×10^{-2}
70	1	0.2	2.70×10^{-2}
70	1	0.4	5.88×10^{-2}
70	1	0.8	1.11×10^{-2}
70	2	0.2	0.250
70	2	0.4	0.500
70	2	0.8	1.00
80	2	0.2	1.50
80	2	0.4	3.00

distributions were obtained; e.g. Figure 3c. Variation of type of particle size distribution with RN is related to rate of sulfide ion generation and its consumption in the growth process (8).

X-ray diffraction spectrum of the ZnS procedure produced from nitrate solutions is given in Figure 4. The pattern is that of sphalerite (11) and there is no evidence of existence of any other crystalline phase. Crystallite size was determined to be on the order of 15 nm by x-ray line broadening technique indicating the polycrystalline nature of spherical particles.

B.2. Sulfate system

ZnS particles formed in sulfate solutions were significantly different in morphology than those formed in nitrate solutions. At low RN values, spherical monosized polycrystalline particles of about 3μm in diameter were formed as shown in Figure 5. X-ray diffraction patterns indicate that the powders consist of both α and β forms of ZnS. No attempt was made to determine the microscopic distributions and the relative amounts of these two phases. The fibrous texture observed for these particles are believed to be due to nuclei that elongated before they attached onto the surface of the growing particles. Similar texture and particle morphology were observed by Williams et al (4). However, they claimed that particles formed by first forming faceted 1 μm cubic crystals followed by the deposition of fibrous crystallites onto the primary crystal. Contrary to

their proposed mechanism, we have not seen any primary crystals in the micron size range. At higher RN values, a second generation of particles appeared after first generation particles reached a diameter of about 3.5 μm, as is shown progressively in Figure 6. Eventually, the second generation particles grew to diameters of 1-2 μm (Figure 6c). It is interesting to note that fibrous texture were more apparent in the second generation of particles, and that the resulting particles were highly agglomerated (Figure 6d). Another significant observation was, that at high RN values, only the β phase (sphalerite) was formed, which suggests that the fibrous features may be associated with the β phase.

B.3. Chloride system

Particles from chloride solutions were very similar to those from nitrate solutions in the range $0.25 < RN < 1.0$ min^{-1}. Monosized, spherical particles with growth rates very similar to those from nitrate solutions were obtained in this range. Figure 7a shows a micrograph of ZnS particles prepared in the presence chloride ions at a temperature of 70°C, pH = 2, $[Zn^{2+}]_o$ = 0.05 M and $[TAA]_o$ = 0.8 M (RN = 1.00). At higher RN values, unlike the nitrate results, chloride solutions did not yield either bimodal or continuous size distributions, probably because effective zinc ion concentration in the solution was diminshed by formation of chloride complexes. Instead, highly agglomerated particles having an average diameter of about 1 μm were obtained as shown in Figure 7b.

B.4. Acetate system

Particle morphology showed only a slight dependence on RN when prepared from acetate solutions. Spherical monosized particles of β-ZnS were obtained with all combinations of experimental variables investigated. Because of buffering, the pH remained fixed at 1.9 and so could not be treated as a variable. Figure 8 shows particles 60 min. after the onset of nucleation under various experimental conditions. A shift in mean particle diameter to larger size is obvious as RN gets lower.

The substructure of particles obtained from acetate solutions was very similar to those from nitrate solutions, i.e., aggregates of nanometer-sized crystallites, as determined from x-ray diffraction line broadening and verified by a specific surface area of about 55 m^2/gr.

Although the low value of S indicates that nucleation kinetics were accelerated in the presence of acetate ions, the growth rate was significantly reduced compared to other anion systems. For example, it took about three hours after nucleation for the particles in Figure 8a to reach a diameter of 0.25 μm.

CONCLUSIONS

Mean ZnS particle size and distribution was affected by the sulfide ion generation rate for all supporting anions except acetate. Depending on the sulfide ion generation rate, monosized, bimodal or continuous size distribution was observed. Nitrate, chloride and acetate solutions produced submicron size particles in the range of variables studied, while sulfate ion solutions produced particles up to 3 μm in diameter. Sulfate ion solutions produced particles that had a fibrous texture which was not apparent in other systems. The unique morphology of the particles produced in the presence of sulfate ions was attributed to complexing of zinc ions with sulfate thus, reducing the rate of nuclei formation compared to other systems. Attachment of sulfate ion onto the growing nuclei to modify the growth habit also cannot be ruled out. Acetate solutions produced very fine (0.1-0.25 μm) spherical monosize particles over a wide range of experimental conditions. Acetate ions appeared to hasten nucleation, yet growth was slow compared to other systems. This phenomenon was attributed to association of acetate and zinc ions to reduce nucleation barrier, resulting in rapid nucleation but little growth.

Powder morphology was more easily controlled in nitrate solutions than with other supporting anions, and the powder characteristics obtained, i.e., size distribution and phase purity, were considered superior to powders obtained with the other anions.

REFERENCES

1. Matijevic, E., J. Coll. Int. Sci. 58(2), 374, 1977.

2. Matijevic, E., Monodispersed Colloidal Metal Oxides, Sulfides and Phosphates, in Ultrastructure Processing of Ceramic Glasses and Composites, Hench, L. L., Ulrich, P. R., Eds., John Wiley & Sons, Inc. (1984).

3. Wilhelmy, D. M. and Matijevic, E., J. Chem. Soc. Faraday Trans., 80, 563, 1984.

4. Williams, R.,Yocom, P. N. and Sotofko, F. S., J. Coll. Int. Sci. 106(2), 388, (1985).

5. Swift, E. H., Butler, E. A., Anal. Chem., 28(2), 146, (1956).

6. King, D. M. and Anson, F. C., Anal. Chem., 33(4), 573, (1961).

7. Akinc, M., Research Proposal Submitted to Office of Naval Research (1986).

8. Celikkaya, A., Akinc, M., Submitted to J. Coll. Int. Sci. (1988).

9. Kotrly, S. and Sucha, L., Handbook of Chemical Equilibria in Analytical Chemistry, p. 143-208, Ellis Hornwood Limited, West Sussex, England, (1985).

10. Gubeli, A. O., and Ste-Marie, J., Can. J. Chem., 45, 2101, (1967).

11. JCPDS X-ray Powder Diffraction File, No. 5-566.

FIGURE CAPTIONS

Figure 1. Change of relative supersaturation with time where T = 60°C, $[TAA]_o$ = 0.4M, pH = 2 and a) $[Zn]_o$ = 0.05M, and b) $[Zn]_o$ = 0.0425M. Times to observe nucleation are indicated with corresponding values of critical relative saturation for acetate, nitrate, chloride and sulfate solutions.

Figure 2. Variation of concentration of thioacetamide as determined a) theoretically, and b) experimentally at pH = 2, $[TAA]_o$ = 0.1M, T = 60°C.

Figure 3. Scanning electron micrographs of ZnS powders obtained from nitrate solutions with $[Zn^{2+}]_o$ = 0.05, pH = 2 and

a) T = 70°C, $[TAA]_o$ = 0.8M.
b) T = 80°C, $[TAA]_o$ = 0.2M.
c) T = 80°C, $[TAA]_o$ = 0.4M.

Figure 4. FTIR spectra of ZnS powders prepared from nitrate solutions.

Figure 5. Scanning electron micrograph of ZnS powders obtained from sulfate solutions at T = 70°C, pH = 1, $[TAA]_o$ = 0.2M and $[Zn^{2+}]_o$ = 0.05M.

Figure 6. Scanning electron micrographs of ZnS powders from sulfate solutions a) 15, b) 30, c) 60, d) 90 min. after precipitation started with T = 70°C, pH = 2, $[TAA]_o$ = 0.4M and $[Zn^{2+}]_o$ = 0.05M.

Figure 7. Scanning electron micrographs of ZnS particles obtained from chloride solutions at pH = 2, T = 70°C, $[Zn^{2+}]_o$ = 0.05M and $[TAA]_o$ = 0.8M.

Figure 8. Scanning electron micrographs of powders obtained from acetate solutions 60 min. after nucleation at $[Zn^{2+}]_o$ = 0.05M, pH = 2 and

a) T = 80°C, $[TAA]_o$ = 0.4M (RN =)
b) T = 60°C, $[TAA]_o$ = 0.8M (RN =)
c) T = 60°C, $[TAA]_o$ = 0.2M (RN =)

Figure 9. X-ray diffracction pattern of ZnS powder obtained in the presence of acetate ions.

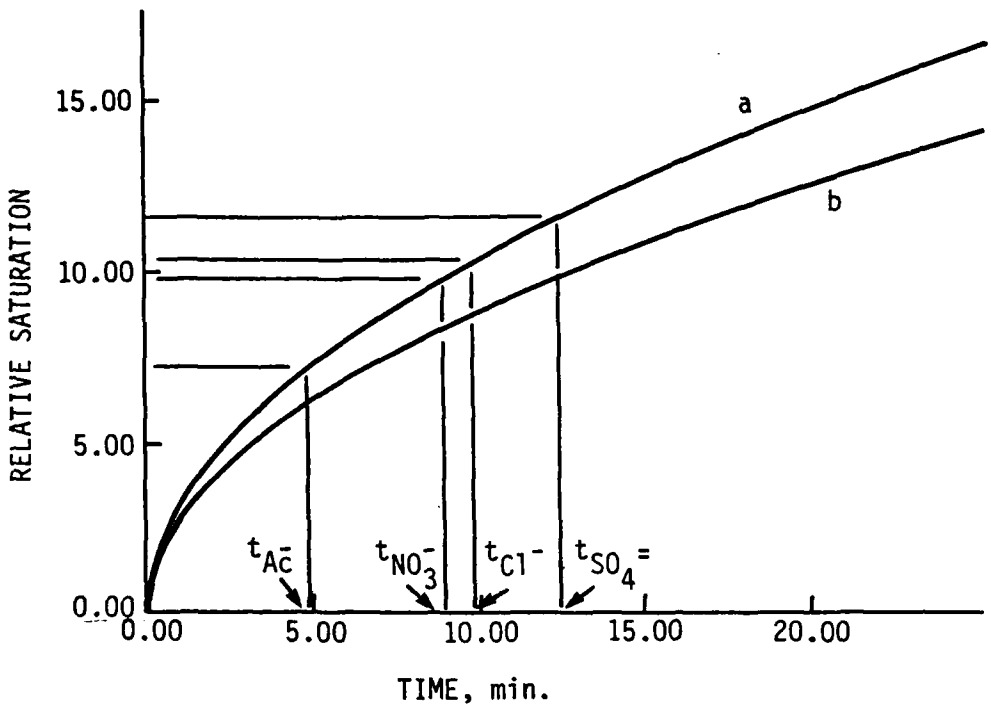

Figure 1 Celikkaya/Akinc

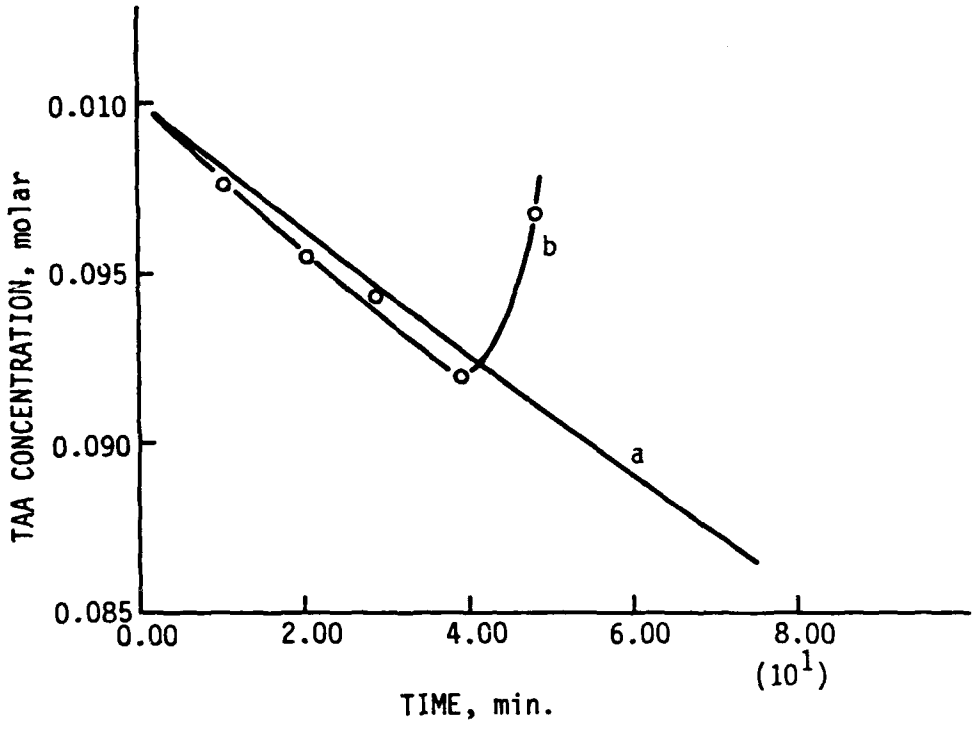

Figure 2 Celikkaya/Akinc

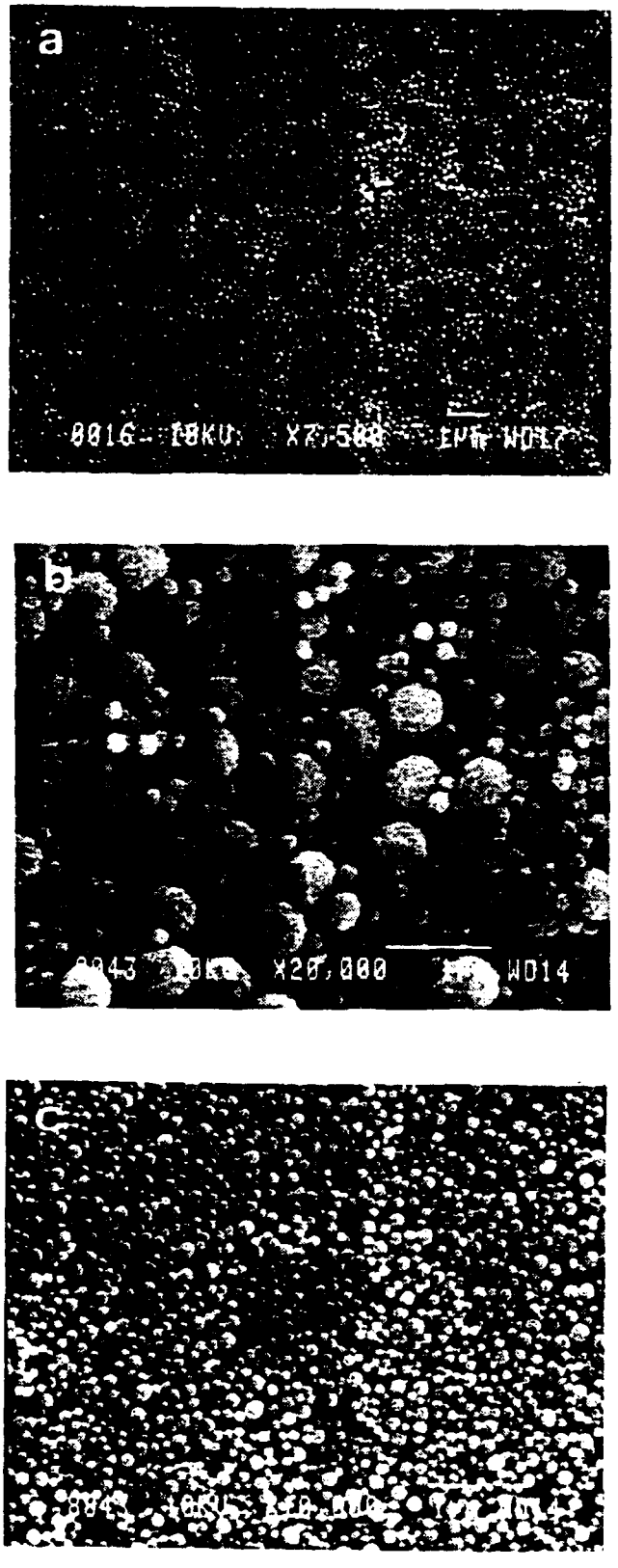

Figure 3 Celikkaya/Akinc

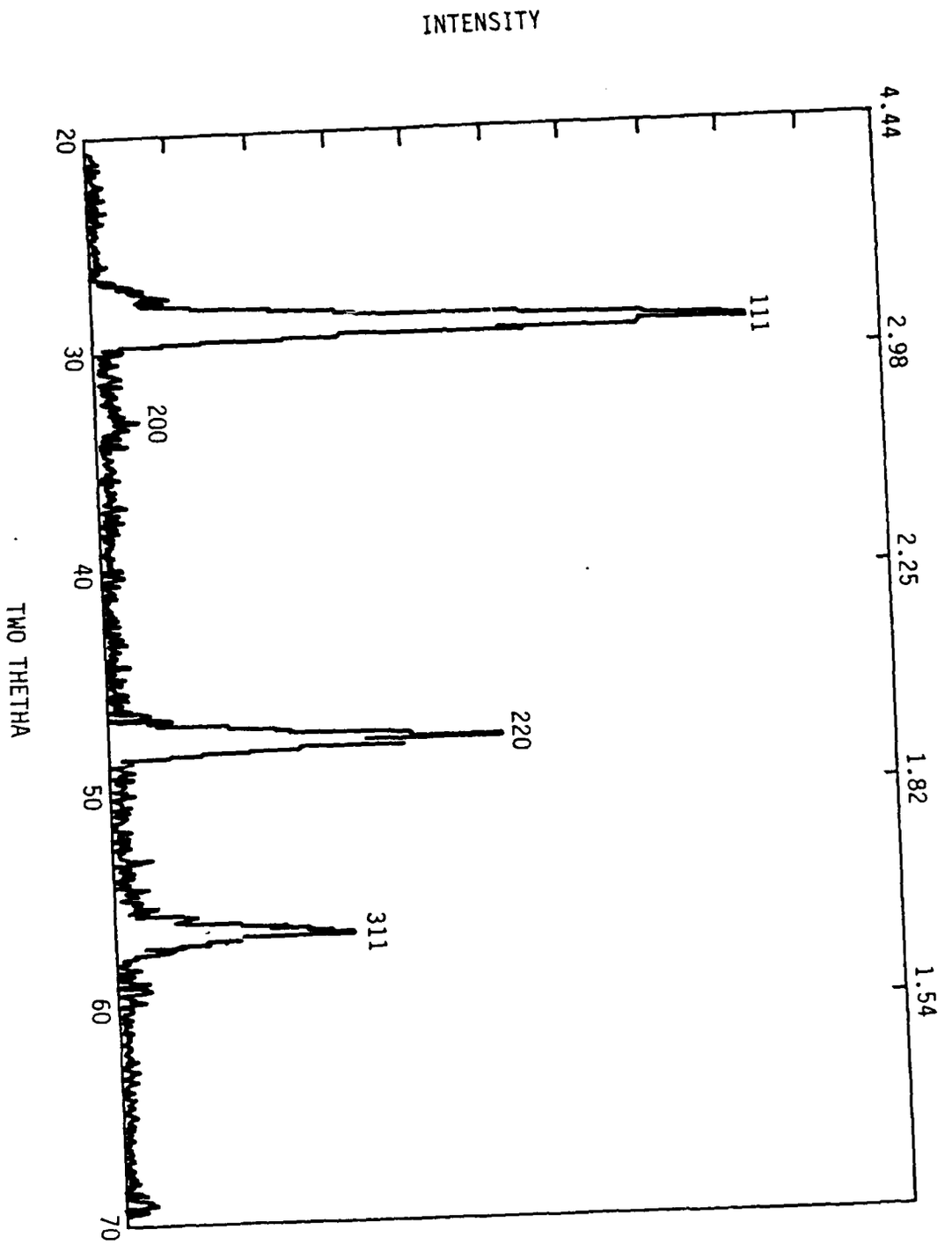

Figure 4 Celikkaya/Akinc

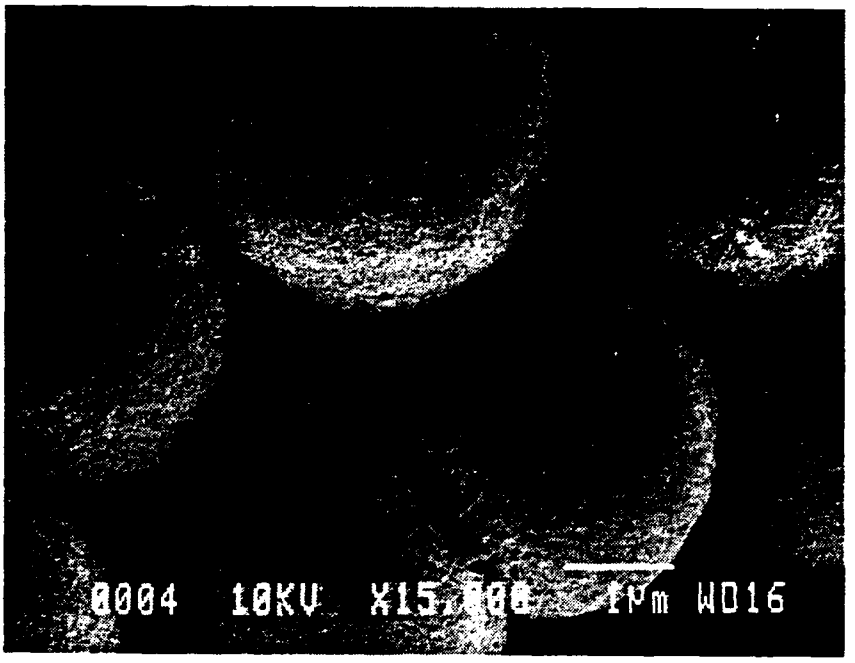

Figure 5 Celikkaya/Akinc

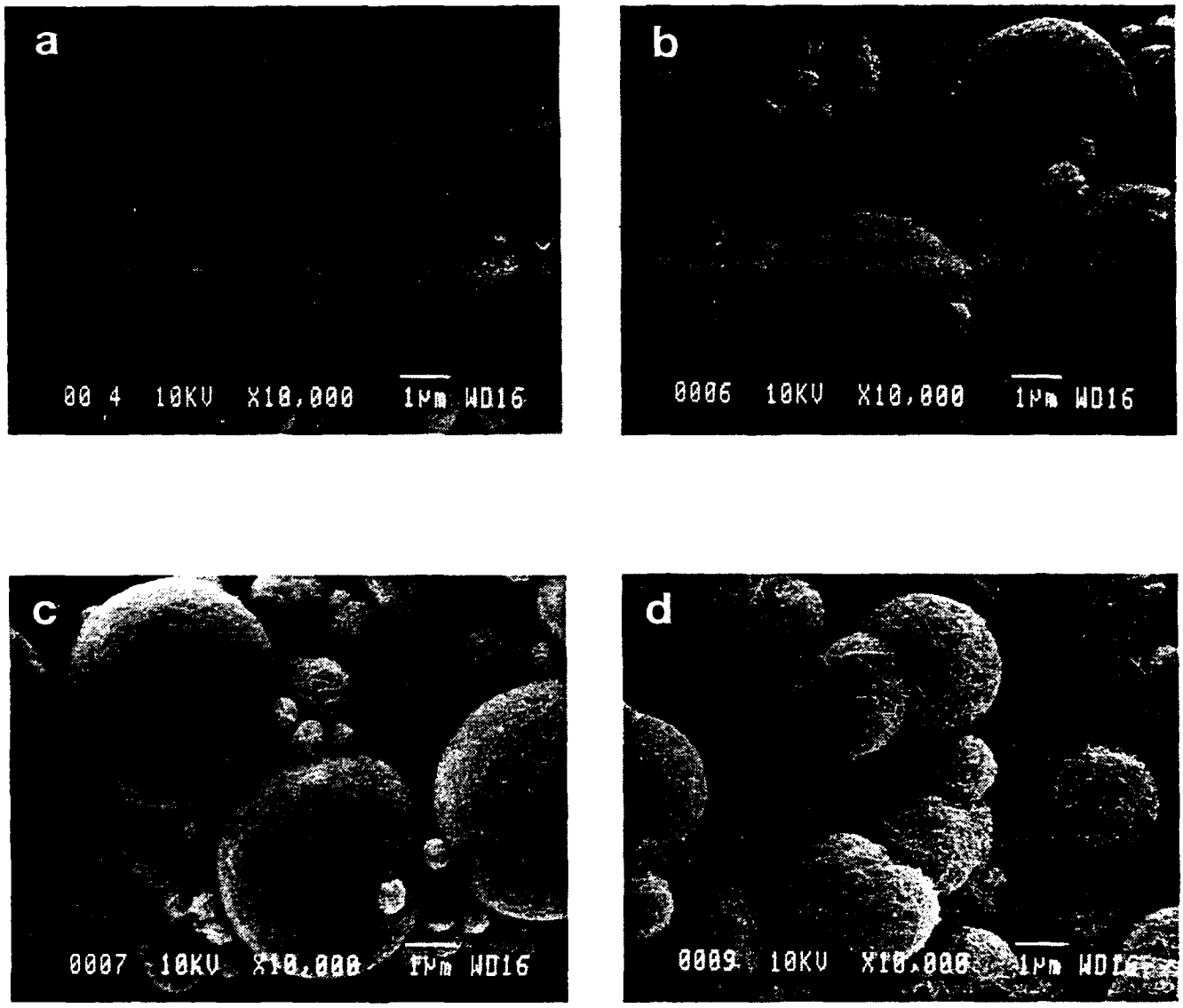

Figure 6 Celikkaya/Akinc

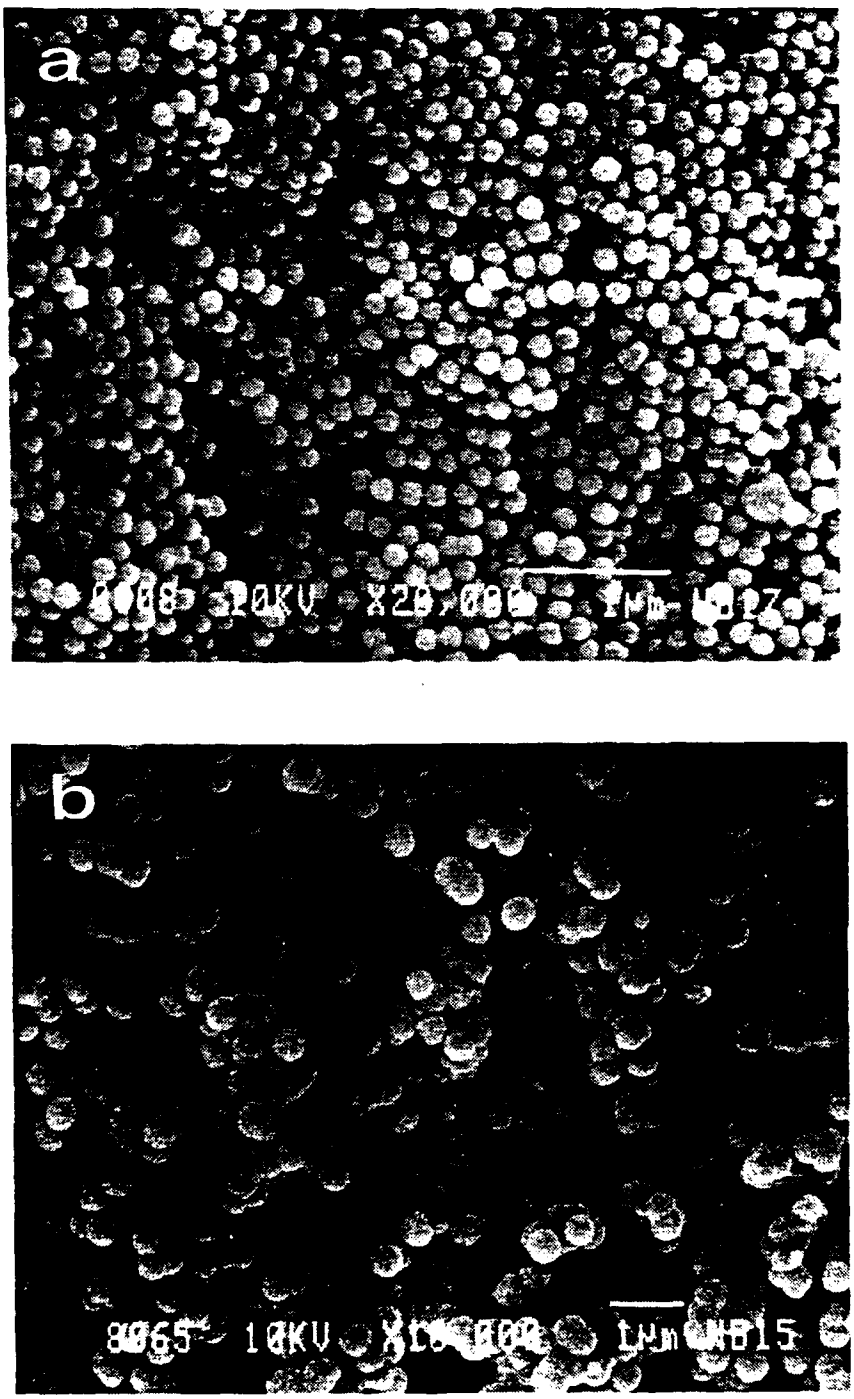

Figure 8 Celikkaya/Akinc

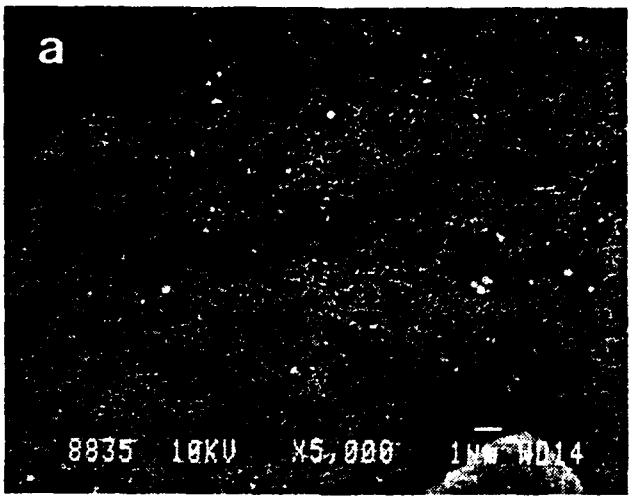

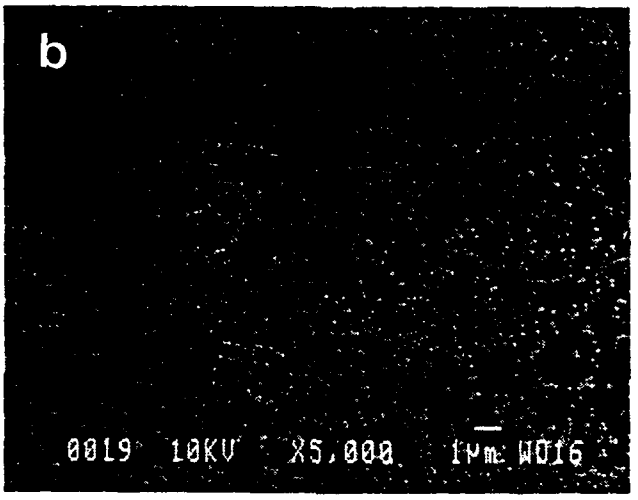

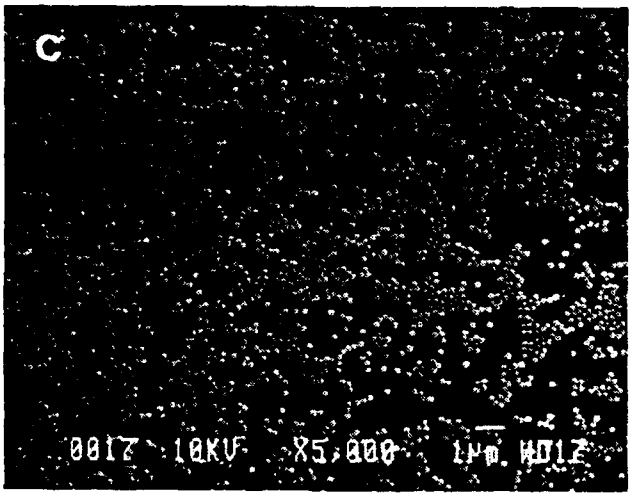

Figure 8 Celikkaya/Akinc

BASIC DISTRIBUTION LIST

Technical and Summary Reports January 1987

Organization	Code	Copies
Defense Documentation Center Cameron Station Alexandria, VA 22314	12	
Office of Naval Research 800 N. Quincy Street Arlington, VA 22217 ATTN: Code 1131 Code 1113		3 1
Naval Air Development Center Code 606 Warminster, PA 18974 ATTN: Dr. J. DeLuccia		1
Commanding Officer Naval Surface Weapons Center 10901 New Hampshire Ave. White Oak Laboratory Silver Spring, MD 20910 ATTN: Mr. W. Messick Code K22		1
Air Force Materials Laboratory Wright-Patterson AFB Dayton, OH 45433 ATTN: Dr. N. Tallan		1
Naval Air Systems Command Code 931A 1411 Jeff Davis Highway Arlington, VA 22202 ATTN: Dr. L. Sloter		1
Defense Metals and Ceramic Information Center Battelle Memorial Institute 505 King Avenue Columbus, OH 43201		1
Naval Weapons Center China Lake, CA 93555 ATTN: Code 385		1
Defense Advanced Research Projects Agency Materials Science Office 1400 Wilson Boulevard Arlington, VA 22209 ATTN: S. Wax		1
Army Research Office P.O. Box 12211 Triangle Park, NC 27709 ATTN: Metallurgy & Ceramics Program Chemistry Program		1 1
Scientific Advisor Commandant of the Marine Corps Washington, DC 20380 ATTN: Code AX		1
Army Materials and Mechanics Research Center Watertown, MA 02172 ATTN: Dr. R. N. Katz		1
Air Force Office of Scientific Research/NE Building 410 Bolling Air Force Base Washington, DC 20332 ATTN: Electronics & Materials Science Directorate		1
Office of Naval Technology 800 N. Quincy Street Arlington, VA 22217 ATTN: Code 0712 Code 0725		1 1

Optical

Dr. Mufit Akinc
Mat'ls Science&Eng.Dept
Iowa State University
110 Engineering Annex
Ames, IA 50011

Dr. H. E. Bennett
Code 38101
Naval Weapons Center
China Lake, CA 93555

Dr. C. Blackmon
Code G23
Naval Surface WeaponsCtr
Dahlgren, VA 22448

Dr. S. Block
Group Leader
Structural Chemistry
National Bureau of Standards
Gaithersburg, MD 20899

Dr. J. Burdett
Chemistry Department
University of Chicago
Chicago, IL 60637

Dr. J. A. Cox
Honeywell Systems and Research
Dept. MN 65-2600
1660 Technology Drive
Minneapolis, MN 55418

Dr. B. Dunn
Materials Science and Engineering Department
Univ. of California, LA
Los Angeles, CA 90024

Dr. G. Geoffroy
Chemistry Department
Pennsylvania State Univ.
University Park,PA 16802

Dr. A. Harker
Rockwell International
P.O. Box 1085
1049 Camino Dos Rios
Thousand Oaks, CA 91360

Dr. D. C. Harris
Code 3854
Naval Weapons Center
China Lake, CA 93555

Dr. R. A. Heinecke
StandardTelecommunication Laboratories, Ltd
London Road
Harlow, Essex CM17 9MA
England

Dr. T. A. Hewston
Code 3854
Naval Weapons Center
China Lake, CA 93555

Dr. M. E. Hills
Code 3854
Naval Weapons Center
China Lake, CA 93555

Dr. Lisa C. Klein
Ctr.forCeramics Research
College of Engineering
Rutgers University
P.O. Box 909
Piscataway, NJ 08854

Dr. P. Klocek
Texas Instruments
P. O. Box 660246
Dallas, TX 75266

Dr. D. N. Lewis
Code 6360
Naval Research Lab
Washington, DC 20375

Ms. D. J. Martin
AFWL/ARBE
Kirtland AFB, NM 87117

Dr. Y. Mehrotra
Perkin-Elmer Company
100 Wooster Heights Road
Danbury, CT 06810

Dr. P. Melling
Ceramics&Glass Technology
Battelle Columbus Labs
Columbus, OH 43201

Dr. R. Messier
Pennsylvania State Univ.
Materials Research Lab
University Park,PA 16802

Ceramics

Dr. G. Messing
Materials Research Dept.
Pennsylvania State Univ.
University Park,PA 16802

Dr. Harry Moreen
Rockwell International
3370 Mira Loma Avenue
Anaheim, CA 92803

Dr. P. E. D. Morgan
Rockwell Science Center
P.O. Box 1085
Thousand Oaks, CA 91360

Dr. S. Musikant
General Electric Co
P. O. Box 8555
Philadelphia, PA 19101

Mr. P. Ormsby
U.S. Army Missile Cmd.
Redstone Arsenal
Huntsville, AL 35807

Dr. C. Pantano
Materials Science Lab
Pennsylvania State Univ.
University Park,PA 16802

Dr. Dale Perry
U.S. Army Missile Cmd.
Redstone Arsenal
Huntsville, AL 35807

Dr. John C. Pulver
Department 144
Eastman Kodak Company
HawkeyePlantApparatusDiv
901 Elmgrove Road
Rochester, NY 14650

Dr. R. Raj
Materials Science and Engineering Department
Cornell University
Ithaca, NY 14853

Dr. W. Rhodes
GTE Laboratories
40 Sylvan Road
Waltham, MA 02134

Mr. R. Rice
W. R. Grace Company
7379 Route 32
Columbia, MD 21044

Mr. D. Roy
Coors Porcelain Company
Golden, CO 80401

Dr. R. Roy
Materials Science Lab
Pennsylvania State Univ.
University Park,PA 16802

Dr. J. Savage
Royal Signals and Radar Establishment
St. Andrews Road
Great Malvern,
WORCS, WR14 3PS
England

Dr. R. W. Schwartz
Code 3854
Naval Weapons Center
China Lake, CA 93555

Dr. A. Stacy
Chemistry Department
Univ. of Calif.,Berkeley
Berkeley, CA 94720

Dr. I. G. Talmy,Code R31
Naval Surface WeaponsCtr
White Oak Laboratory
Silver Spring, MD 20903

Mr. W. Tropf
Applied Physics Lab
Johns Hopkins Road
Laurel, MD 20810

Dr. R. Tustison
Raytheon Co.Research Div
131 Spring Street
Lexington, MA 02173

Dr. W. White
Materials Research Lab
Pennsylvania State Univ.
University Park,PA 16802

Dr. A. Wold
Chemistry Department
Brown University
Providence, RI 02912